Chapter 8

$\mathrm{D_S^+}$ and $\mathrm{D^+}$ mesons reconstruction in Pb–Pb collisions

The work presented in this Thesis so far has focused on the study of the $\mathrm{D_s^+/D^+}$ production-yield ratio in pp collisions at $\sqrt{s} = 13.6$ TeV, which can provide information on a possible production of small QGP droplets in small collision systems. However, the main goal of the ALICE experiment is the study of heavy-ion collisions, where an extended deconfined phase is expected to be formed. Measurements of $\mathrm{D_s^+}$-meson production in Pb–Pb collisions have been performed by the ALICE Collaboration at the centre-of-mass energies per nucleon-nucleon collision of $\sqrt{s_{\mathrm{NN}}} = 5.02$ TeV [1, 2] and $\sqrt{s_{\mathrm{NN}}} = 2.76$ TeV [3]. The measured R_{AA} of prompt $\mathrm{D_s^+}$ mesons in Pb–Pb collisions is compatible within uncertainties with that of other non-strange D mesons ($\mathrm{D^0}, \mathrm{D^+}$, and $\mathrm{D^{*+}}$) for $p_{\mathrm{T}} \gtrsim 10\mathrm{GeV}/c$, where the hadronisation process is expected to occur mainly via fragmentation. At lower p_{T}, where the coalescence mechanism is expected to play a more relevant role, the measured R_{AA} of prompt $\mathrm{D_s^+}$ mesons is systematically higher than that of non-strange D mesons, although the results are compatible within one standard deviation. In addition, while the measured production-yield ratio of non-strange over non-strange D mesons ($\mathrm{D^+/D^0}$ and $\mathrm{D^{*+}/D^0}$) is found to be compatible in Pb–Pb and pp collisions, indicating no significant modification of their relative abundances as a function of p_{T} and centrality, the production-yield ratio of strange over non-strange D mesons ($\mathrm{D_s^+/D^+}$ and $\mathrm{D_s^+/D^0}$) is found to be larger in Pb–Pb collisions than in pp collisions, but the measurements in the two systems are compatible within about one standard deviation. The large uncertainties of the measurements in Pb–Pb collisions do not allow for drawing firm conclusions on the production mechanism of $\mathrm{D_s^+}$ mesons in heavy-ion collisions.

Thanks to the upgrade of the ALICE detector during the LHC Long Shutdown 2, the experiment significantly improved its readout rate in Pb–Pb collisions to more than 50 times the one achieved during the LHC Run 2 data-taking period [4]. This will allow for enhancing the precision of the measurements of rare probes, such as heavy-flavour hadrons, and for completely new insights into the properties of the QGP, such as the exclusive reconstruction of beauty-hadron decays. With the improvements in the detector capabilities, the strange over non-strange D-meson production-yield ratios can be measured with unprecedented precision in Pb–Pb col-

lisions, providing more significant evidence, or the lack thereof, of the phenomenon of strangeness enhancement in the QGP.

At the time of starting the work presented in this Thesis, the ALICE Collaboration was performing the first collisions of ultra-relativistic lead ions with the upgraded apparatus. Therefore, rapid feedback on the quality of the data was required. Since the upgrade of the ALICE detector mainly focused on the improvement of its capabilities for heavy-flavour measurements, particular attention was given to the performance of the reconstruction of D mesons. Hence, the first studies carried out for this Thesis aimed at the reconstruction of D mesons in Pb–Pb collisions. In this Chapter, the analysis strategy and the results of the reconstruction of $\mathrm{D_s^+}$ and $\mathrm{D^+}$ mesons in Pb–Pb collisions at $\sqrt{s_{\mathrm{NN}}} = 5.36$ TeV are presented.

8.1 Event selection and data sample

The analysis reported in this Chapter is performed on a dataset of Pb–Pb collisions at a centre-of-mass energy of $\sqrt{s_{\mathrm{NN}}} = 5.36$ TeV, collected by the ALICE detector during the 2023 data-taking period. Since the calibration of the track reconstruction was still ongoing at the time of the analysis, and because the reconstruction of Pb–Pb events is very resource-intensive, only a fraction of 20% of the total data sample collected during the 2023 data-taking period was made available and therefore analysed. Only once the quality of the reconstruction of Pb–Pb events was validated, the full dataset was processed.

The data sample is collected using a Minimum-Bias trigger (the `Sel8` trigger), which selects events that satisfy the requirement of having a signal coincidence in the FT0-A and FT0-C detectors. The centrality of the collision is determined using the forward-rapidity FT0-C detector. The centrality classes are defined as percentiles of the charged-particle multiplicity distribution (which is calibrated for each data-taking period), starting from the events with higher multiplicity. Therefore, collisions in the 0–10% centrality class are the most central, with the largest number of produced charged particles.

The analysed centrality classes are the 10–30%, 30–50%, and 60–90%, but no signal is extracted in the last centrality class.

8.2 $\mathrm{D_s^+}$ and $\mathrm{D^+}$ mesons reconstruction

$\mathrm{D_s^+}$ and $\mathrm{D^+}$ mesons are reconstructed in the same decay channel exploited for the measurement of the $\mathrm{D_s^+/D^+}$ production-yield ratio in pp collisions presented in the previous Chapters:

$$\mathrm{D_s^+, D^+ \to \phi\pi^+ \to K^+K^-\pi^+} \quad .$$

In the most central Pb–Pb collisions, around 21500 charged particles are produced on average [5]. Therefore, the reconstruction of D mesons in ultra-relativistic heavy-ion collisions is more challenging than in pp collisions since a much larger combinatorial background from the combination of three uncorrelated tracks is produced. On the other hand, the higher particle production in Pb–Pb collisions allows for a better reconstruction of the primary vertex, and, thereby, a slight improvement in the

separation of the signal from the background, by exploiting the displaced decay topology of the D mesons, is achieved.

An additional difficulty to the reconstruction of D-meson signals is represented by the fact that a completely new analysis framework was developed for the LHC Run 3 data-taking period, to cope with the continuous readout of the detector. The reconstruction of D mesons, therefore, helped to validate the new framework and to provide feedback on its performance.

Furthermore, with the replacement of the TPC MultiWire Proportional Chambers readout chambers with Gas Electron Multipliers performed during the LHC Long Shutdown 2 upgrade, the amount of backflow of ions in the TPC has significantly increased. The residual ions in the TPC gas volume can distort the electric field, leading to a distortion of the drift paths of the ionised electrons. This effect is particularly relevant in the track reconstruction, as it worsens the momentum resolution and the track reconstruction efficiency. Despite a great effort in the calibration of the TPC, the backflow of ions is still present and affects the track reconstruction. This leads to a more difficult reconstruction of D_s^+ and D^+ mesons, as the broadening of their signal peaks due to the non-optimal momentum resolution may lead to an overlap of their invariant mass distributions given the small mass difference of about 10 MeV/c^2.

Lastly, at the time this work was carried out, Monte Carlo simulations of Pb–Pb collisions enriched with heavy-flavour hadrons were not available. Therefore, there was no possibility of employing Machine Learning (ML) techniques to select the D-meson candidates, as it is done for the analysis of the D_s^+/D^+ production yield ratio in pp collisions described in the previous Chapters, since a pure data sample of signal candidates needed to train the ML model could not be obtained.

Therefore, the selection of D-meson candidates is performed using rectangular selection criteria exploiting the displaced decay topology of heavy-flavour hadrons and their decay kinematic. Additionally, particle identification techniques of the decay products are employed to reduce the combinatorial background and select D_s^+ and D^+ candidates. Selections based on the same variables used in the pp analysis, described in Chapter **??** are applied. Since the number of particles produced in a heavy-ion collision varies drastically with the centrality of the collision, the selection criteria employed for the selection of D-meson signals were optimised independently for each centrality class.

For each centrality interval, the selection criteria are optimised by maximising the statistical significance of the extracted D_s^+-meson signal on a set of predefined variables, for each considered p_T interval. This strategy is used as no physics observables are meant to be extracted from the analysis, and the main goal is to validate the reconstruction framework and provide feedback on its performance. In fact, the maximisation of the statistical significance of the signal should not be pursued as a strategy for the selection of D-meson candidates in physics analyses, as statistical fluctuations can lead to a bias in the extracted yields.

The variable space considered for the optimisation of the set of selection criteria employed for the selection of D_s^+ and D^+ meson candidates is reported in Table 8.1, where the variables used, the considered variation range, and the number of intermediate steps are reported. A total of 1728 selection criteria were considered for

Table 8.1: Variation range and number of steps for the variables used in the optimisation of the selection criteria for the selection of D_s^+- and D^+-meson candidates in Pb–Pb collisions at $\sqrt{s_{NN}} = 5.36$ TeV.

			p_T (GeV/c)				
Variable	N. steps		2–4	4–6	6–8	8–12	12–24
$L(\mu m) >$	3	min	200	200	200	200	200
		max	600	800	800	800	800
$\cos\theta_p >$	4	min	0.990	0.998	0.998	0.980	0.980
		max	0.9990	0.9995	0.9995	0.9950	0.9950
$\cos\theta_p^{xy} >$	4	min	0.990	0.997	0.998	0.980	0.980
		max	0.9990	0.9985	0.9995	0.9950	0.9950
$\lvert\Delta M(KK)\rvert(MeV/c^2) <$	3	min	5	5	5	5	5
		max	9	9	9	9	9
$\lvert\cos^3(\theta'(K))\rvert >$	3	min	0.1	0.1	0.1	0.1	0.1
		max	0.3	0.3	0.3	0.3	0.3
$\chi^2_{PCA} <$	4	min	3	3	3	3	3
		max	12	12	12	12	12

each p_T interval of the different centrality classes. In addition to those reported in Table 8.1, a few variables are used to further improve the selection of D_s^+ and D^+ mesons, but their thresholds are not optimised. The normalised decay length in the transverse plane is required to be larger than 2, and the PID information $|n\sigma|$ of the three daughter tracks from both the TPC and TOF detectors is required to be at most equal to 4. As for the analysis performed in pp collisions, the information from the TOF detector was used when available, but not required.

Figure 8.1 illustrates the results for the optimisation of the D_s^+ meson statistical significance in the 10–30% centrality class for the 2–4 GeV/c p_T interval. The large modulations of the statistical significance dividing the graph into three parts are due to the different thresholds applied to the candidate decay length. Smaller periodic modulations of the D_s^+ statistical significance are also observed and are due to the different thresholds applied to the other considered variables.

The optimal selection criteria for the selection of D_s^+ meson candidates in the 10–30% and 30–50% centrality classes are reported in the Tables 8.2 and 8.3, respectively. The optimal selection criteria for the 60–90% centrality class are not reported, as no signal was extracted in this centrality class.

8.3 Signal extraction

Once the selection criteria are optimised for each p_T interval and centrality class, the signal is extracted by fitting the invariant mass distribution of the selected candidates. The fit function is composed of an exponential function for describing the background shape and two gaussian functions for the D_s^+ and D^+ signal. The fit of the invariant mass distributions of the candidates passing the selection criteria described above is performed in the invariant mass range of $1.7 < M < 2.1$ GeV/c^2.

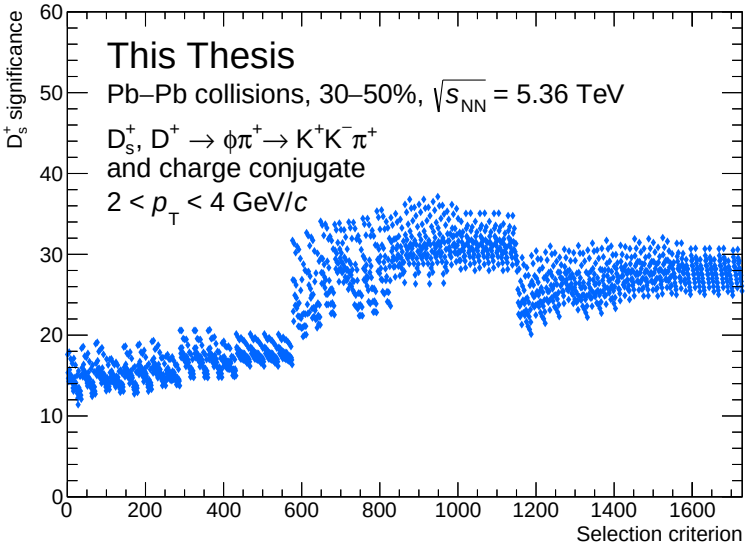

Figure 8.1: D_s^+-meson signal statistical significance as a function of the selection criteria for the $2 < p_T < 4$ GeV/c interval in the 30–50% centrality class.

Table 8.2: Optimal selection criteria for the selection of D_s^+ meson candidates in the 10–30% centrality class.

	p_T interval (GeV/c)				
Variable	2−4	4−6	6−8	8−12	12−24
$L(\mu m) >$	600	200	500	200	200
$\cos\theta_p >$	0.99	0.998	0.9985	0.98	0.98
$\cos\theta_p^{xy} >$	0.999	0.998	0.998	0.99	0.995
$\lvert\Delta M(KK)\rvert(MeV/c^2) <$	7	9	5	7	7
$\lvert\cos^3(\theta'(K))\rvert >$	0.3	0.2	0.2	0.2	0.3
$\chi^2_{PCA} <$	3.0	6.0	3.0	3.0	9.0

Extraction of the signal is achieved in both the 10–30% and 30–50% centrality classes, with statistical significances ranging from 14 to 35 for D_s^+ mesons and from 4 to 14 for D^+ mesons in the first centrality interval, and from 9 to 37 for D_s^+ mesons and from 4 to 21 for D^+ mesons in the 30–50% centrality class. Figure 8.2 shows the normalised invariant mass distribution of D-meson candidates passing the applied selections in the 10–30% centrality class and $2 < p_T < 4$ GeV/c interval (left panel) and in the 30–50% centrality class and $4 < p_T < 6$ GeV/c interval (right panel).

As mentioned above, one of the consequences of the backflow of ions in the TPC is the distortion of the drift paths of the ionised electrons, which leads to a worsening of the track momentum resolution. These effects can be observed already in Fig. 8.2: while the D_s^+ and D^+ peaks are well separated in both the $2 < p_T < 4$ GeV/c and $4 < p_T < 6$ GeV/c intervals, in this last p_T interval the peak widths are larger, and the separation between the two peaks is less pronounced. Therefore, to test the validity of the distortion corrections in the reconstruction framework it is important to study the resolution of the D_s^+ and D^+ mesons peaks.

Table 8.3: Optimal selection criteria for the selection of D_s^+ meson candidates in the 30–50% centrality class.

Variable	p_T interval (GeV/c) 2−4	4−6	6−8	8−12	12−24
$L(\mu m) >$	400	200	200	200	200
$\cos\theta_p >$	0.996	0.998	0.998	0.98	0.995
$\cos\theta_p^{xy} >$	0.996	0.997	0.998	0.985	0.98
$\lvert\Delta M(KK)\rvert(MeV/c^2) <$	7	9	9	5	5
$\lvert\cos^3(\theta'(K))\rvert >$	0.1	0.1	0.1	0.1	0.2
$\chi^2_{PCA} <$	3.0	3.0	12.0	12.0	9.0

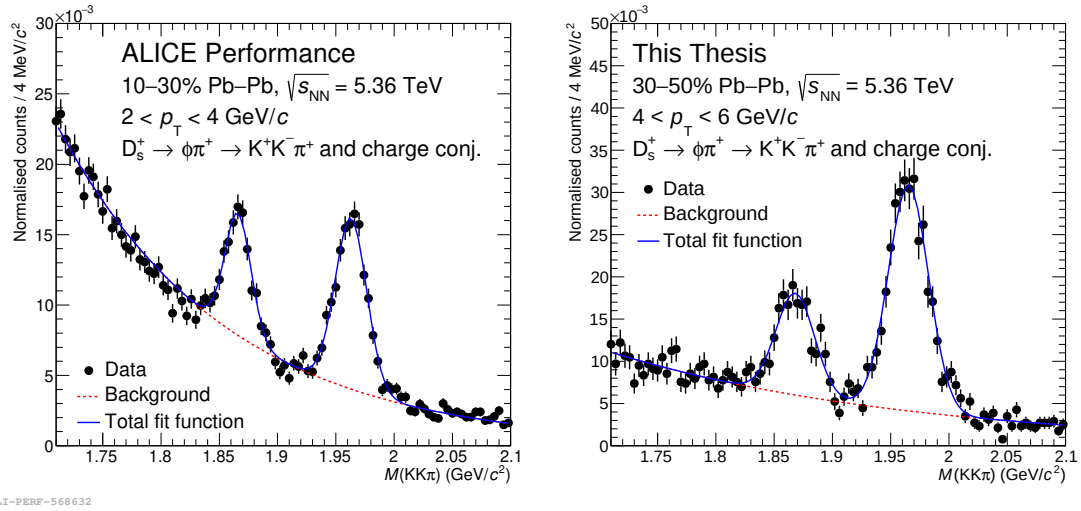

Figure 8.2: Normalised invariant mass distribution of the selected D-meson candidates in the 10–30% centrality class and $2 < p_T < 4$ GeV/c interval (left panel) and in the 30–50% centrality class and $4 < p_T < 6$ GeV/c interval (right panel).

The resolution of the D_s^+ and D^+ mesons peaks is extracted from the fits of the invariant mass distribution of the selected candidates as the standard deviation of the gaussian distribution used to describe the D-meson signals. In Figure 8.3, the peak width of the D_s^+ meson signal is shown for the analysis performed in this Thesis using the 30–50% centrality class of Pb–Pb collisions recorded in the LHC Run 3 data-taking period (blue markers) as a function of p_T. A clear increasing trend of the peak width with p_T is observed, and is attributed to the worsening of the momentum resolution due to the distortions of the electric field in the TPC. This is also indicated by the smaller peak widths of the D_s^+-meson signals extracted from the Pb–Pb collisions data collected during the LHC Run 2 data-taking period at $\sqrt{s_{NN}} = 5.02$ TeV in the 30–50% centrality class [1], when the TPC ion backflow was significantly suppressed using active gating grids. Those results, shown with green markers in Fig. 8.3, were obtained employing ML algorithms to extract D-meson signals, and present a milder dependence on p_T. Lastly, the peak widths of the D_s^+-meson signals extracted from pp collisions data recorded during the LHC

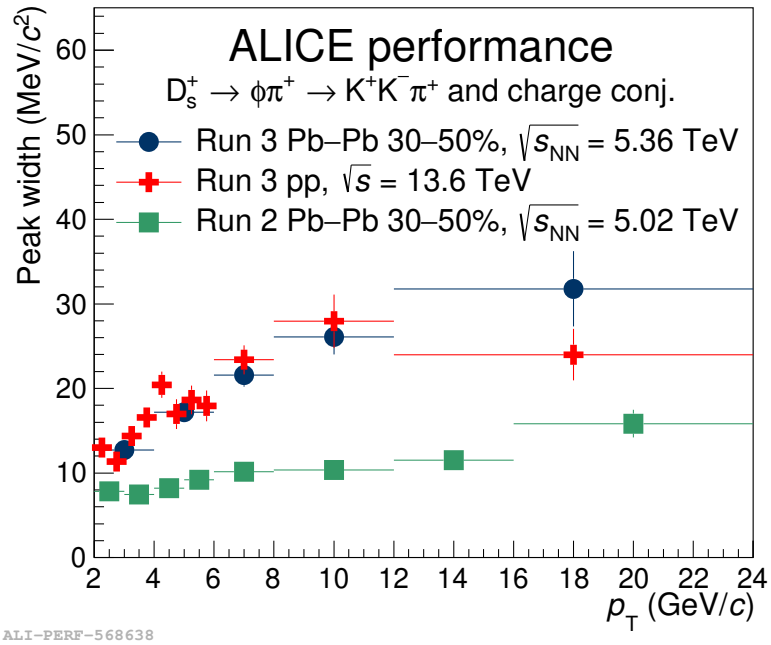

Figure 8.3: Width of the D_s^+-meson signal peak as a function of p_T measured in Pb–Pb collisions at $\sqrt{s_{NN}} = 5.36$ TeV in the 30–50% centrality class and pp collisions at $\sqrt{s} = 13.6$ TeV recorded during the LHC Run 3 data-taking period (blue and red markers, respectively) and in the 30–50% centrality class of Pb–Pb collisions at $\sqrt{s_{NN}} = 5.02$ TeV recorded during the LHC Run 2 data-taking period (green markers).

Run 3 data-taking period at $\sqrt{s} = 13.6$ TeV are reported as a function of p_T with red markers. Although the values of the D_s^+-meson peak widths from pp collisions are not used for the final results reported in Chapters **??** and **??**, they are from an initial analysis that used a similar strategy to extract the raw yields of the D_s^+ and D^+ mesons, employing ML algorithms to separate signal and background candidates. These results show a trend with p_T which is consistent with what is observed from the measurements performed with data from the LHC Run 3 data-taking period in Pb–Pb collisions at $\sqrt{s_{NN}} = 5.36$ TeV, confirming that the observed worsening of the momentum resolution is due to the backflow of ions in the TPC.

Bibliography

[1] **ALICE** Collaboration, S. Acharya *et al.*, "Measurement of prompt $\mathrm{D_s^+}$-meson production and azimuthal anisotropy in Pb–Pb collisions at $\sqrt{s_{\mathrm{NN}}} = 5.02$ TeV", *Phys. Lett. B* **827** (2022) 136986, arXiv:2110.10006 [nucl-ex].

[2] **ALICE** Collaboration, S. Acharya *et al.*, "Measurement of $\mathrm{D^0}$, $\mathrm{D^+}$, $\mathrm{D^{*+}}$ and $\mathrm{D_s^+}$ production in Pb-Pb collisions at $\sqrt{\mathrm{s_{NN}}} = 5.02$ TeV", *JHEP* **10** (2018) 174, arXiv:1804.09083 [nucl-ex].

[3] **ALICE** Collaboration, J. Adam *et al.*, "Measurement of $\mathrm{D_s^+}$ production and nuclear modification factor in Pb-Pb collisions at $\sqrt{\mathrm{s_{NN}}} = 2.76$ TeV", *JHEP* **03** (2016) 082, arXiv:1509.07287 [nucl-ex].

[4] **ALICE** Collaboration, "ALICE upgrades during the LHC Long Shutdown 2", arXiv:2302.01238 [physics.ins-det].

[5] **ALICE** Collaboration, J. Adam *et al.*, "Centrality dependence of the pseudorapidity density distribution for charged particles in Pb-Pb collisions at $\sqrt{s_{\mathrm{NN}}} = 5.02$ TeV", *Phys. Lett. B* **772** (2017) 567–577, arXiv:1612.08966 [nucl-ex].